Continuous-wave singly resonant optical parametric oscillator pumped by a single-frequency resonantly doubled Nd:YAG laser

S. T. Yang, R. C. Eckardt, and R. L. Byer

Edward L. Ginzton Laboratory, Stanford University, Stanford, California 94305

Received December 30, 1992

We report what is to our knowledge the first demonstration of a continuous-wave singly resonant optical parametric oscillator based on potassium titanyl phosphate. The pump source used is a single-frequency resonantly doubled Nd:YAG laser. By double passing the pump through the crystal, we achieved a minimum oscillation threshold of 1.4 W. With 3.2 W of incident pump power, a maximum 1.07 W of nonresonant idler power was generated. Spectral measurement reveals that the singly resonant optical parametric oscillator operates consistently in a single axial mode with much relaxed axial mode hop tolerance to cavity length and pump-frequency fluctuations compared with doubly resonant optical parametric oscillators previously demonstrated.

Significant progress has been made on the performance of cw optical parametric oscillators (OPO's). By use of improved pump sources, such as diode-pumped solid-state lasers, and new nonlinear materials, cw doubly resonant OPO's have been operated with high efficiency and narrow linewidth.[1,2] However, the simultaneous requirements for phase matching and coincidence of signal and idler resonances in satisfying conservation of energy place severe tolerance limits on cavity length and pump-frequency fluctuations.[3,4] The stringent tolerances can be relaxed by resonating only the signal or idler in the OPO cavity.[5] Unfortunately, the higher threshold of the singly resonant OPO (SRO) has hampered its development, and only pulsed SRO's, pumped by Q-switched or continuously mode-locked lasers, have been operated to date.[6] For applications such as high-resolution laser spectroscopy and optical-frequency division, however, a truly continuous source with single-frequency output and narrow linewidth is desirable. In this Letter we report what is to our knowledge the first experimental demonstration of a cw SRO pumped by a single-frequency source.

The SRO setup is illustrated in Fig. 1. The single-frequency pump source consists of an injection-locked Nd:YAG laser that routinely produces 12 W of power at 1064 nm in the TEM_{00} mode with a 20-kHz linewidth.[7] The output from the injection-locked laser is resonantly doubled in an external enhancement cavity containing a 6-mm-long LiB_3O_5 crystal to produce 4 W of cw power at 532 nm.[8]

The nonlinear crystal used in the SRO is potassium titanyl phosphate (KTP). KTP is chosen as the OPO crystal because it has a large nonlinearity, low absorption loss at the signal and idler wavelengths, a large temperature-acceptance bandwidth, and a high damage threshold that can withstand the high pump intensity necessary to reach threshold. The 10-mm-long KTP crystal is oriented for propagation along a crystallographic axis (i.e., $\theta = 90°$, $\phi = 0°$). The parametric interaction utilizes type II noncritical phase matching. The 532-nm pump beam is polarized along the y axis of the crystal and propagates along the x axis. The signal and idler waves generated at 1090 and 1039 nm are polarized along the y and z axes, respectively.[9] The KTP crystal is placed at the intracavity focus of a three-mirror standing-wave resonator consisting of two 5-cm radius-of-curvature mirrors (M1, M2) and one flat mirror (M3). Mirror M2 is mounted upon a piezoelectric transducer for fine adjustment of cavity length. To reduce astigmatism, the incident angle on mirror M1 is set at 3°. With a calculated signal-beam waist radius of 31 μm and a measured pump-beam waist radius of 21 μm, the signal and pump beams have confocal parameters (b_s, b_p) that equal the crystal length. All mirrors are highly reflecting ($R > 99.9\%$) over the range extending from 970 to 1160 nm and highly transmitting at 532 nm ($T > 98\%$). The crystal has dual-band antireflection

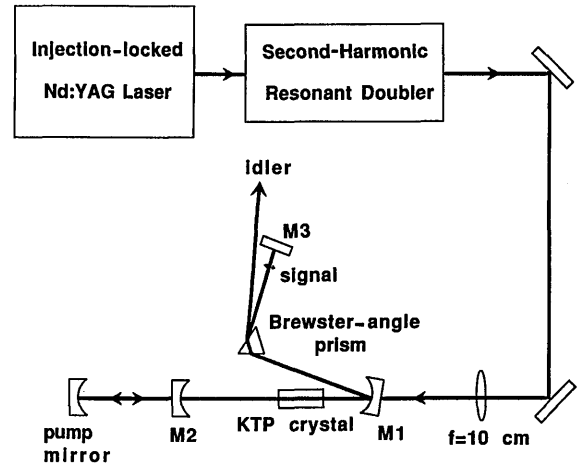

Fig. 1. KTP SRO experimental setup. The spacing between the two curved mirrors is 8.2 cm. The distance from mirror M1 to mirror M3 is 14 cm. Both the pump mirror and mirror M2 are mounted upon piezoelectric transducers. The $LiNbO_3$ prism with an apex angle of 48.3° has its c axis coming out of the page.

0146-9592/93/120971-03$6.00/0

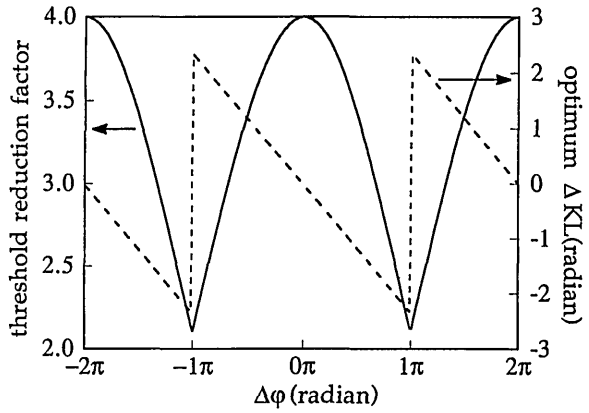

Fig. 2. Double-pass threshold reduction with both pump and idler nonresonantly reflected as a function of relative phase difference $\Delta\phi$ (solid curve). At each $\Delta\phi$, ΔkL is optimized to yield maximum threshold reduction. For $\Delta\phi$ varying between $-\pi$ and π, the optimum ΔkL varies between +2.33 and −2.33 rad (dashed curve).

coatings centered at 1090 and 532 nm. To ensure that only the signal at 1090 nm is resonant, we place a Brewster-angle $LiNbO_3$ prism in the long leg of the cavity to spatially separate the signal and idler beams. The prism is cut so that the signal beam goes through the prism polarized along the ordinary axis of $LiNbO_3$, whereas the idler beam traverses the prism polarized along the extraordinary axis. Because of the large difference in refractive index between ordinary and extraordinary axes of $LiNbO_3$, the signal and idler beams emerge from the prism separated by 8°, allowing the idler beam to be rejected completely out of the SRO cavity.

The finesse of the SRO cavity is 743 at 1064 nm, which implies a round-trip power loss of 0.85%. The actual loss at the signal wavelength of 1090 nm is expected to be less, because the antireflection coating is centered at 1090 nm. With this loss figure, the expected cw SRO threshold with a single-pass pump can be calculated by using the threshold formula given in Ref. 10. For calculating threshold, we assume $d_{\text{eff}} = 3$ pm/V for KTP[9,11,12] and that both the pump and signal beams are confocally focused inside the crystal (i.e., $b_s = b_p = L$). For crystal length $L = 1$ cm and a round-trip signal power loss of 0.85%, the calculated SRO threshold is 7.2 W.

To lower the threshold, a 25-cm radius-of-curvature mirror that is highly reflecting at 532 nm is mounted on a piezoelectric transducer and placed after mirror M2 to retroreflect the pump beam back through the crystal. As was pointed out by Bjorkholm *et al.*,[13] reflecting the pump and the idler nonresonantly back through the crystal can reduce the SRO threshold by as much as a factor of 4. However, because all three waves are present on the return pass through the crystal, the net parametric gain and therefore the threshold reduction are dependent on the relative phase difference between the three waves after reflection and before the second pass through the crystal. For instance, if the relative phase difference changes by π after reflection so that the pump-wave phase now leads rather than lags the combined signal and idler phase by $\pi/2$ on the second pass through the crystal, the parametric gain obtained in the first pass will be canceled during the second pass, and the threshold will be infinite at $\Delta kL = 0$, where ΔkL is the momentum mismatch. The relative phase difference will change from its initial value before reflection because of momentum mismatch in the crystal, difference in mirror phase shift suffered on reflection, and dispersion of air. Also, because the pump beam and the signal plus idler beams are reflected by separate mirrors, the phase shift between the three waves differs by the difference in the path lengths traveled. Here, we denote the change to relative phase difference aside from momentum mismatch by $\Delta\phi$. Assuming nonresonant pump and idler reflection, we can express the double-pass pump threshold as

$$P_{\text{th-DP}} = \frac{P_{\text{th-SP}}}{[1 + R_p + 2\sqrt{R_i R_p}\cos(\Delta\phi + \Delta kL)]} \times \left[\frac{\sin^2(\Delta kL/2)}{(\Delta kL/2)^2}\right]^{-1}, \quad (1)$$

where SP and DP denote single- and double-pass pumps, R_i is the idler-power reflection coefficient of mirror M2, and R_p is the pump-power reflection coefficient of the pump mirror. When $\Delta\phi \neq 0$, the minimum threshold does not occur at $\Delta kL = 0$. Figure 2 shows a plot of threshold reduction versus $\Delta\phi$, assuming perfect reflection of pump and idler (i.e., $R_i = R_p = 1$). At each $\Delta\phi$, ΔkL is optimized to yield the maximum threshold reduction. As is shown in Fig. 2, the threshold for the double-pass pump SRO can be 4–2.1 times less than the threshold for a single-pass SRO, depending on the change in relative phase difference after reflection. The minimum threshold is achieved after every 2π change in $\Delta\phi$. To illustrate this threshold dependence on change in relative phase, we recorded SRO output as the pump phase or varied the combined signal plus idler phases by moving the position of either the piezo-mounted pump mirror or mirror M2. Figure 3 shows the case when the pump-mirror position is varied while mirror M2 is held fixed. We see that SRO goes above threshold at every 2π pump-phase shift

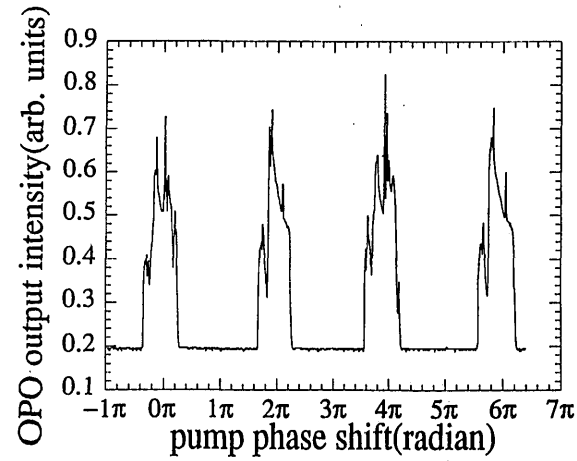

Fig. 3. SRO output as the pump mirror position is swept. Mirror M2 is held fixed. A pump-phase shift of 2π corresponds to a pump-mirror motion of 266 nm.

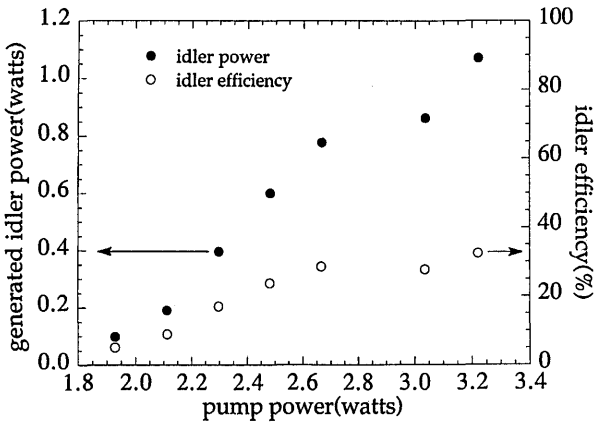

Fig. 4. SRO nonresonant idler output power and power conversion efficiency versus input pump power. The filled circles refer to the generated idler power, and the open circles represent idler power conversion efficiency.

corresponding to 266 nm of mirror motion. Similar behavior is observed when the pump mirror is held fixed while the position of mirror M2 is swept.

With optimum relative phase, a double-pass cw SRO threshold of 1.4 W was measured. Assuming perfect mode matching and unity reflectance for pump and idler waves, the threshold is reduced by a maximum of four times, and the single-pass threshold is inferred to be 5.6 W. This would imply an upper-bound round-trip signal loss of 0.66%, which is reasonable compared with the round-trip loss of 0.85% measured at 1064 nm. Figure 4 shows a plot of SRO idler output power and conversion efficiency versus input-pump power. The idler power plotted is extrapolated from actual power measured after the prism by taking into account the 62% reflection loss of the *s*-polarized idler wave from the prism's two surfaces. This reflection loss can be eliminated, in principle, and the total idler power generated can be coupled out in a single beam. With 3.2 W of pump input, the maximum idler power generated was 1.07 W. The corresponding signal output was 12 mW from each of the three cavity mirrors. The combined signal-plus-idler output power conversion efficiency was 34.6%. Pump depletion was observed to be 61% with 2.85 W of incident pump power. At this pumping level, the total idler power was 861 mW. This represents a pump-to-idler power conversion efficiency of 30.2% and an idler output coupling efficiency of 97%. The high output coupling efficiency was expected because the output coupling loss through the prism dominates the <1% residual loss from the crystal's antireflection coating. The generated idler beam has a Gaussian-like spatial distribution. Owing to beam expansion through the prism, the output idler beam is elongated with an aspect ratio of 1.28:1.

Coarse tuning of the KTP SRO can be accomplished in principle by varying the crystal phase-matching angle. Because the KTP crystal is 90° noncritically phase matched, tuning is insensitive to change in the crystal angle. More than 5° of rotation (internal angle) in either the xz plane (θ axis) or the xy plane (φ axis) is necessary for any noticeable wavelength change to be achieved.[9,14] Experimentally, no significant wavelength tuning was achieved by tuning the crystal angle because the SRO quickly goes below threshold as one moves away from collinear noncritical phase-matching condition.

With only one wave resonant, the frequency stability of the SRO should be much less susceptible to cavity-length or pump-frequency fluctuations than for doubly resonant OPO's. Indeed, as observed with a 300-MHz free-spectral-range scanning Fabry–Perot interferometer, the SRO ran consistently in a single axial mode even though the cavity is made up of discrete components and the setup is exposed to laboratory environment. The linewidth of the idler was measured to be the scanning Fabry–Perot instrument resolution of a few megahertz, and it is potentially as narrow as the pump linewidth of 20 kHz. To confirm the less stringent axial-mode hop tolerance, pump frequency was swept over 40 MHz, and no axial mode hop was observed. This contrasts with the 3-MHz pump-frequency fluctuation tolerance for a similar-length doubly resonant OPO.[3,4]

In conclusion, a cw KTP SRO has been successfully operated. The SRO produces as much as 1.07 W of idler and 36 mW of signal-output power with 3.2 W of pump input, representing a total OPO output power conversion efficiency of 34.6%. The SRO exhibits excellent spectral purity with consistent single-axial-mode operation, and it is much less susceptible to cavity-length and pump-frequency perturbations than the doubly resonant OPO's previously operated. The demonstrated high efficiency and narrow linewidth of the cw SRO should make it an attractive source for high-resolution laser spectroscopy and optical-frequency division applications.

This research was supported by U.S. Office of Naval Research grant N00014-92-J-1903 and a grant from the Sony Corporation.

References

1. C. D. Nabors, R. C. Eckardt, W. J. Kozlovsky, and R. L. Byer, Opt. Lett. **14,** 1134 (1989).
2. D. Lee and N. C. Wong, Opt. Lett. **17,** 13 (1992).
3. R. G. Smith, IEEE J. Quantum Electron. **QE-9,** 530 (1973).
4. R. C. Eckardt, C. D. Nabors, W. J. Kozlovsky, and R. L. Byer, J. Opt. Soc. Am. B **8,** 646 (1991).
5. S. E. Harris, Proc. IEEE **57,** 2096 (1969).
6. For a recent review of pulsed SRO's, see C. L. Tang, W. R. Bosenberg, T. Ukachi, R. J. Lane, and L. K. Cheng, Proc. IEEE **80,** 365 (1992).
7. C. D. Nabors, A. D. Farinas, T. Day, S. T. Yang, E. K. Gustafson, and R. L. Byer, Opt. Lett. **14,** 1189 (1989).
8. S. T. Yang, C. C. Pohalski, E. K. Gustafson, R. L. Byer, R. S. Feigelson, R. J. Raymakers, and R. K. Route, Opt. Lett. **16,** 1493 (1991).
9. K. Kato, IEEE J. Quantum Electron. **27,** 1137 (1991).
10. S. Guha, F. J. Wu, and J. Falk, IEEE J. Quantum Electron. **QE-18,** 907 (1982).
11. R. C. Eckardt, H. Masuda, Y. X. Fan, and R. L. Byer, IEEE J. Quantum Electron. **26,** 922 (1990).
12. H. Vanherzeele and J. D. Bierlein, Opt. Lett. **17,** 982 (1992).
13. J. Bjorkholm, A. Ashkin, and R. G. Smith, IEEE J. Quantum Electron. **QE-6,** 797 (1970).
14. K. Kato and M. Masutani, Opt. Lett. **17,** 178 (1992).